Experimental Investigation on a Finite-Span Circular Cylinder with Tangential Blowing

by

Fumio Yoshino* and Ryoji Waka*

(Received June 30, 1979)

The experimental investigation has been carried out to inquire into the flow around a finite-span circular cylinder with tangential blowing. It was found that the flow was three-dimensional almost over the whole span as far as the used model is concerned. The flow separated from the cylinder surface extremely early near the tip and root of the model. The boundary layer control by means of jet-blowing is extremely difficult there, especially near the tip. The performance of the finite-span cylinder with blowing was found to be poor.

1 Introduction

Up to date there are many investigations concerning the flow around the circular cylinder with blowing in two-dimensional flow. They are very important to obtain the fundamental data appling to a lift-augmented airfoil, film cooling, fluidics and so on.

However many of the flow around an object in practice separate from the surface of it and are three-dimensional. The reason is thought to be caused by the shape and finiteness of the span of the object.

Hence, the flow field, where the jet is blown into the separated and three-dimensional flow, is profoundly interesting to investigate experimentally. Also it is significant to investigate the effects of the tip and root of the cylinder on the flow around it because of difficulty of estimating the degree of those effects theoretically.

In this report, we describe the experimental results obtained by using a finite-span circular cylinder with tangential blowing of air in uniform flow.

2 Nomenclatures

B = Span of the model ;

* Department of Mechanical Engineering

C_d = Total drag coefficient $\left(= \dfrac{(\text{Drag})}{1/2 \rho_\infty U_\infty^2 DB} \right)$;

C_l = Total lift coefficient $\left(= \dfrac{(\text{Lift})}{1/2 \rho_\infty U_\infty^2 DB} \right)$;

C_p = Static-pressure coefficient $\left(= \dfrac{P_s - P_\infty}{1/2 \rho_\infty U_\infty^2} \right)$;

C_μ = Momentum coefficient of jet $\left(= \dfrac{Mh}{1/2 \rho_\infty U_\infty^2 D} \right)$;

D = Diameter of the cylinder ;

h = Width of the slot ;

M = Momentum of jet at the outlet of the slot ;

P_s = Static-pressure on the cylinder surface ;

P_∞ = Static-pressure in the wind tunnel ;

R_e = Reynolds number $\left(= \dfrac{U_\infty D}{\nu_\infty} \right)$;

z = Distance from the mid-span in spanwise direction (the starboard is plus) ;

θ = Angle measured clockwise from the leading edge (Fig. 2) ;

θ_j = Angular position of the slot ;

θ_p = Angular position of the static-pressure hole measured clockwise from the slot ;

λ = Aspect ratio ;

ρ_∞ and ν_∞ = Density and kinematic viscosity coefficient of air in the wind tunnel,
respectively.

3   Experimental installment and method

The assembly drawing of the model
is shown in Fig. 1. The model consists
of a vertically wide and streamlined
body, two circular cylinders and a
supporting system.   The span of the
model is 571 mm and the body is in-
stalled at the mid-span of the model.
This body has dimensions of 60 mm in
width, 713 mm in length and 360 mm
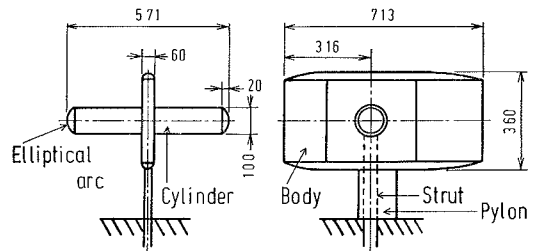in height.   The hollow strut is con-

Fig. 1 Assembly drawing of the model.

nected to the body and is fixed on the three-component balance below the tunnel floor after passing through it.

The compressed air, stored in an air-tank, is supplied equally into insides of the cylinders on both sides of the body through the strut and is blown downstream as jet from the slot along a cylinder surface. The width of this slot is constant, 0.55 mm, over the span from | 2z/B | = 0.105 to 0.930. The tips of the model are not sharp edge but elliptical arc for air to flow smoothly around there.

The cross-section of circular cylinders used in this experiment is shown in Fig. 2. The sectional shape has the same size and structure as that already used.[1] The model has 150 static-pressure holes, in all, on the cylinder surface circumferencially distributed at various spanwise sections as shown in Table I.
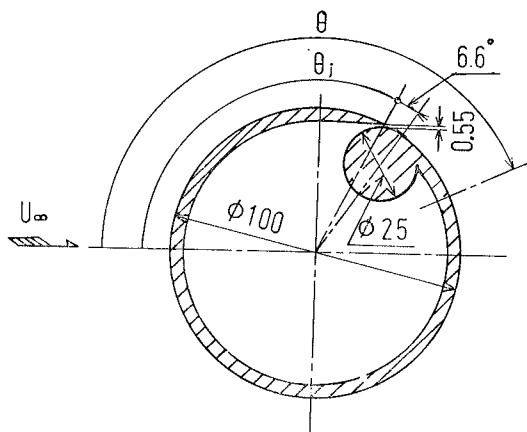

Fig. 2 Cross-section of the cylinder.

Table I Angular and spanwise positions of the static-pressure holes.

Row	2z/B	θp°
3	0.834	6.6, 16.6, 26.6, 36.6, 46.6, 56.6
6	0.557	66.6, 76.6, 86.6, 96.6, 106.6, 116.6
9	0.196	231.6, 241.6, 256.6, 261.6, 271.6, 281.6 291.6, 301.6, 311.6, 321.6
1	0.911	
2	0.893	
4	0.778	6.6, 16.6, 26.6, 36.6
5	0.708	46.6, 56.6, 66.6, 76.6
7	0.382	86.6, 96.6, 106.6, 116.6
8	0.266	
10	0.119	

The performance of the wind tunnel used for the experiment is described in the reference 2), and is not repeated here. The experimental conditions are shown in Table II.

The measurements of aerodynamic force, total lift and drag acting on the

Table II Experimental conditions.

θj°	Re x10⁵	Cμ	
90	1.92	0, 0.10, 0.30, 0.50, 0.74, 0.86, 1.00	
90	2.56	0, 0.10, 0.22, 0.30, 0.50, 0.62, 0.74	
105	3.20	0, 0.02, 0.04, 0.06, 0.08, 0.10, 0.14	
		0.22, 0.26, 0.32, 0.34, 0.42, 0.46	

model were made by means of three-component balance. These measured values include the drag of the pylon and the reaction force caused by the blown jet. The drag acting on the pylon was determined by applying the momentum theorem to the measured velocity profile in the wake of the pylon. The value of this drag was subtracted from the value of the drag measured by means of the balance.

The circumferencial and spanwise static-pressure distributions on the cylinder

surface were measured to determine the characteristic values and to investigate the flow near the tip and root of the model. Moreover the visualization of the stream-line on the cylinder surface was made by means of oil-flow method. It is useful to know the flow around the cylinder intuitively.

4   Results and Discussion

The circumferential static-pressure distributions on the cylinder surface at three spanwise sections are shown in Fig. 3. The distributions at the rows of No. 3 and 9 vary so much in the rear part of the cylinder. It is found that the static-pressure gradient is very large at each spanwise section, especially at the rows of No. 3 and 9, and the separation of flow is early in the neighborhoods of the tip and root of the model. Also the drops of the static-pressure are shown downstream the separation points at the rows of No. 3 and 9. It is thought that these drops are due to the vortices trailing downstream from the cylinder surface. This is described later. The flow around the cylinder seems no longer to be two-dimensional almost over the whole span.

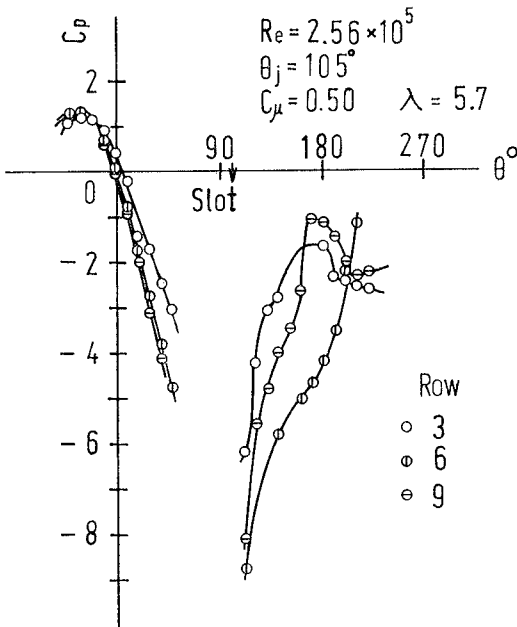The relations between C_l, C_d and

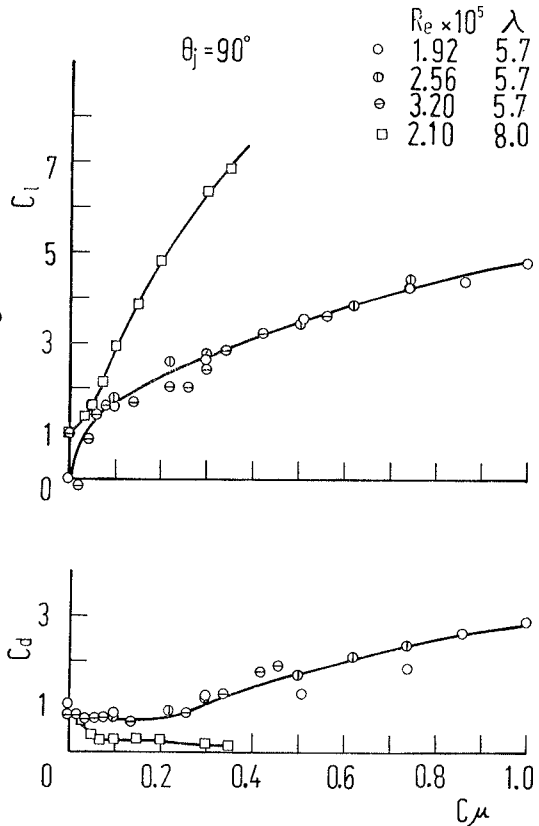Fig. 3 Static-pressure distributions around
          the cylinder.

Fig. 4 Relations between C_l, C_d and C_μ.

C_μ are shown in Fig. 4. The values of C_l and C_d are determined respectively from total lift and drag of the model measured by means of the balance. The square symbols in this figure indicate the values determined from the static-pressure distributions at the mid-span of the cylinder which spanned the whole width of the wind tunnel with aspect ratio of 8. These values are corrected by considering the thrust due to the blown jet and approximately regarded as the values in two-dimensional flow.

The larger the C_μ is, the larger the value of C_l is. The relation is monotonous. However, the rate of increase of C_l against C_μ is very small compared with that in two-dimensional flow.

On the other hand, when C_μ becomes large, C_d becomes very large compared with the value of C_d in two-dimensional flow. It is expected from this result that the large induced drag is acting on the cylinder.

Therefore the values of C/C_d are very small in the case of the finite-span cylinder (Fig. 5).
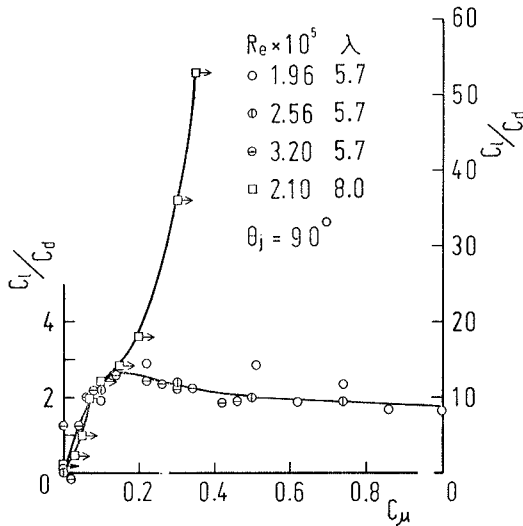

Fig. 5 Relation between C_l/C_d and C_μ.

Fig. 6 Polar diagram of lift and drag.

The polar diagram of lift and drag is shown in Fig. 6. The performance of this model as a wing is not so good. It is also found that the large induced drag is acting on the cylinder.

The reason of this poor performance is thought that C_l and C_d are the mean values over the whole span and they are influenced by the three-dimensional effect due to the tip and root of the model.
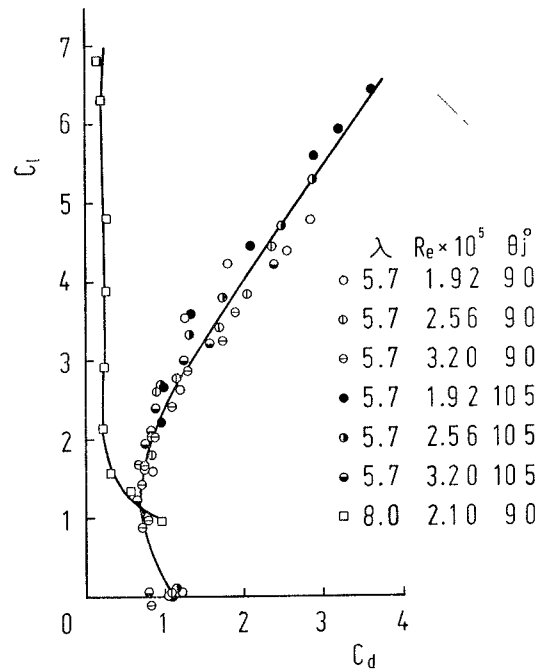
In Figs. 4, 5 and 6 the difference due to R_e is not recognized and the scattering of data seems to be within experimental error.
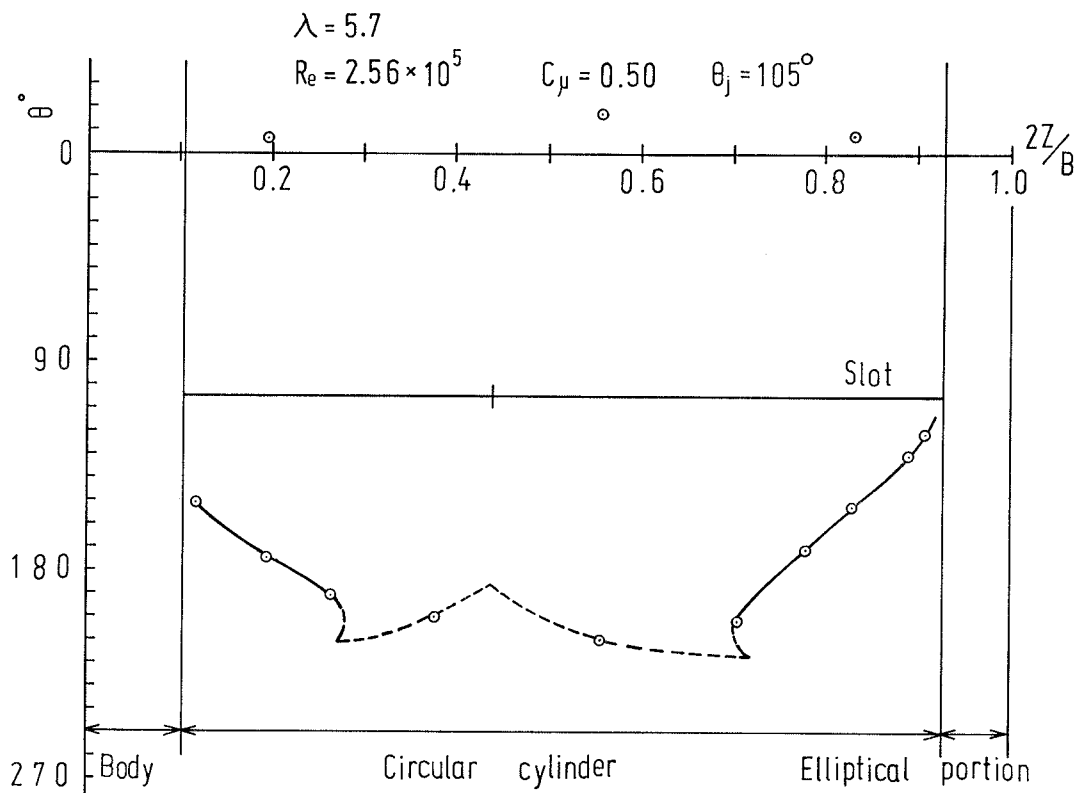

Fig. 7   Separation line on the cylinder surface.

The spanwise separation line on the cylinder surface is shown in Fig. 7. The symbols indicate the separation points obtained from the circumferential static-pressure distributions on the cylinder surface and the dotted line indicates the separation line obtained by making reference to the result of the oil-flow method (see Fig. 8).

It is found from these figures that the separation of flow is comparatively early in the neighborhoods of the tip and root, and two strong vortices rolling in opposite directions each other are formed on the cylinder surface. The early separation near the root is caused by the interference of the boundary layer developed on the surface of the body and cylinder.

On the other hand, the flow at the tip of the cylinder seems to separate just downstream of the slot. The jet blown from the slot has much mometum. But the surrounding air is entrained into the part between the jet and the cylinder surface
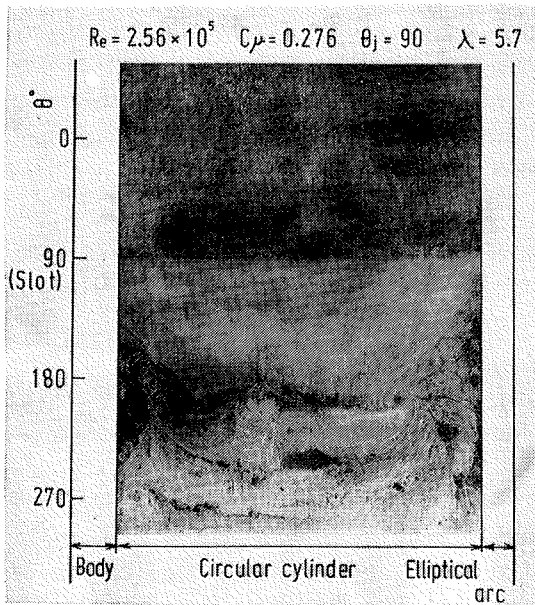
Fig. 8 Oil-flow line on the cylinder surface.

from the tip. This entrained flow cancels out Coanda effect. Hence the threedimensionality of the flow near the tip is more grown than that near the root.

The flow at the section of $2z/B=0.44$ branches away in two ways. It is caused by a stay set in the inside of the slot to keep the slot-width constant.

The flow around the finite-span circular cylinder is three-dimensional almost over the whole span in this way. Howevr it may be thought that the flow is more likely two-dimensional in the neighborhood of $2z/B = 0.5$ if the model without a stay is used.
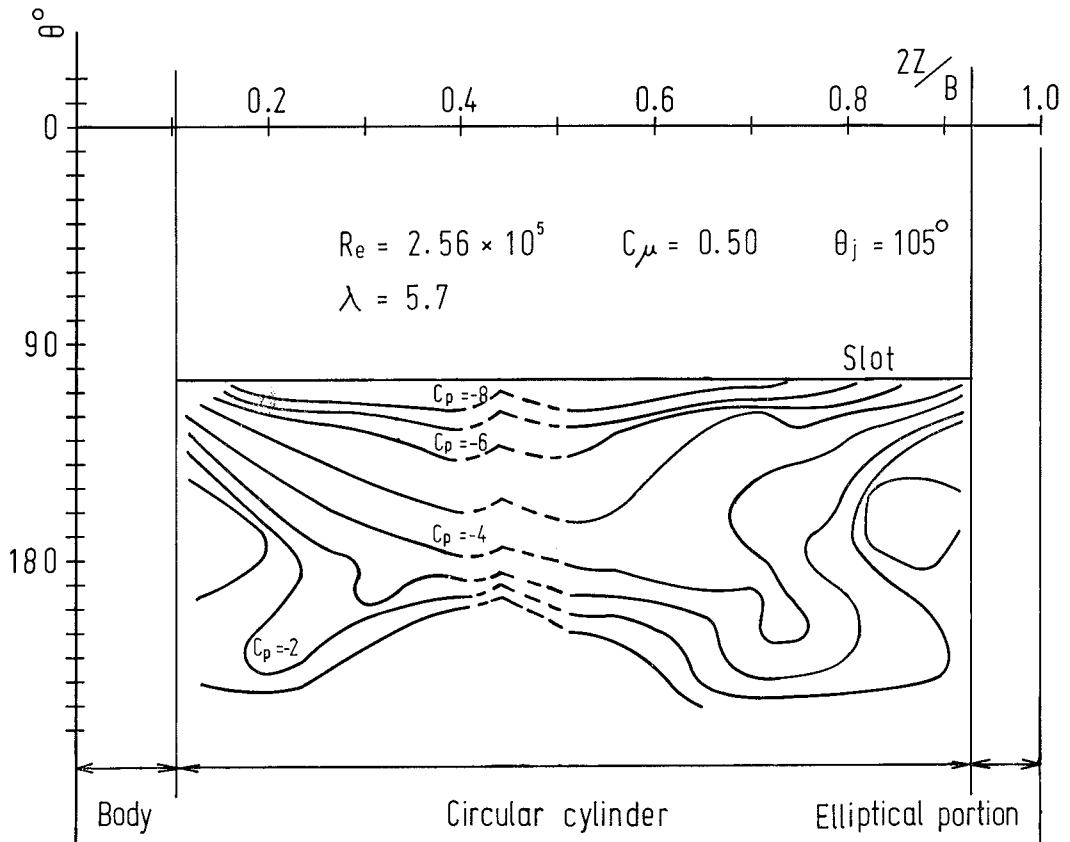
The equi-static-pressure lines on the

Fig. 9 Equi-static-pressure lines on the cylinder surface.

cylinder surface are shown in Fig. 9. These lines are not straight but wavy almost ovre the whole span. The dotted lines indicate some uncertainty because they are drawn by making reference to Fig. 8. The adverse pressure gradient is strong just downstream of the slot in the neighborhoods of the tip and root. There are two portions of low static-pressure in the neighborhoods of the tip and root in the regions of $\theta \fallingdotseq 200°$. They are corresponding to the results mentioned above, that is, there are two vortices trailing downstream, rolling in opposite directions each other.

5 Concluding remarks

The flow around a finite-span circular cylinder is three-dimensional almost over the whole span in this model. The tip-effect is more dominant than the effect of the body. The stay set inside of the slot also has an effect on the flow outside of the slot.

As a whole, the performance of the finite-span cylinder with blowing is very poor, which suggests that the total drag includes large induced drag.

Reference

1) Yoshino and Waka, Reports of the Faculty of Engineering of Tottori University, 3–2 (1973–3)
     25.
2) Yoshino and the other, Reports of the Faculty of Engineering of Tottori University, 1–1
     (1970–12), 7.